BIOCHEMISTRY
including biophysical chemistry & molecular biology

Article

pubs.acs.org/biochemistry

Molecular Basis for the Inhibition of HMGA1 Proteins by Distamycin A

Austin E. Smith and Karen L. Buchmueller*

Department of Chemistry, Furman University, Greenville, South Carolina 29613, United States

Supporting Information

ABSTRACT: The molecular mechanism for the displacement of HMGA1 proteins from DNA is integral to disrupting their cellular function, which is linked to many metastatic cancers. Chemical shift and NOESY NMR experiments provide structural evidence for the displacement of an AT hook peptide (DNA binding motif of HMGA1 proteins) by both monomeric and dimeric distamycin. However, the displaced AT hook alters distamycin binding by weakening the distamycin:DNA complex, while slowing monomeric distamycin dissociation when AT hook is in excess. The central role of the AT hook was evaluated by monitoring full-length HMGA1a protein binding using fluorescence anisotropy. HMGA1a was effectively displaced by distamycin, but the cooperative binding exhibited by distamycin was eliminated by displaced HMGA1a. Additionally, these studies indicate that HMGA1a is displaced from the DNA by 1 equiv of distamycin, suggesting the ability to develop therapeutics that take advantage of the positively cooperative nature of HMGA1a binding.

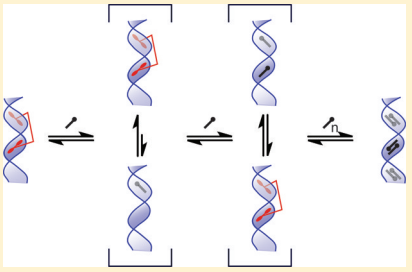

Malignant neoplasms are one of the leading causes of death in the United States.[1] Thus, disrupting the function of proteins that are linked with these cancers is a viable target for small molecule therapies.[2] Members of the High Mobility Group A1 (HMGA1) protein family have been detected at high concentrations in a wide variety of cancers, and overexpression is associated with different cancers including pancreatic,[3,4] thyroid,[5] and breast.[6−10] HMGA1 proteins are essential for embryogenesis,[11,12] but expression of these proteins in healthy adult tissues is low to undetectable.[5,12] In particular, the upregulation of HMGA1 proteins has been linked to tumor metastasis and correlates with poor prognosis for the patient.[5,13−18] Silencing of the HMGA1 gene by RNA interference, in a mouse model system, effectively inhibits metalloproteases and downregulates cell proliferation, tumor migration, and invasion.[19] The larger family of HMGA proteins regulates an array of nuclear functions,[13,17,20] and their high degree of flexibility is implicated in a variety of mechanisms that control gene expression, such as recruitment of transcription factors to DNA and alteration of DNA architecture.[13,17,20−22] These proteins are characterized by the occurrence of multiple DNA binding motifs, called AT hooks, that preferentially bind AT-rich DNA. The work herein focuses on one of the human proteins, HMGA1a, and a peptide analogue comprised of one of the three AT hook motifs.[23]

HMGA1 proteins are intrinsically disordered prior to binding DNA[24] and as a result are difficult to target directly; therefore, targeting the DNA sequences that HMGA1a binds has greater potential for downregulating protein activity.[25,26] To effectively target such a multifarious and flexible protein, it is essential to understand the dynamics of HMGA1a inhibition by using a readily available small molecule, such as distamycin A or Hoechst 33258, both of which have been shown to displace HMGA from DNA.[27] Toward this goal, we have structurally characterized the dynamic inhibition of both the AT hook and the full-length HMGA1a protein binding to DNA by the small molecule, distamycin A. This naturally occurring polyamide preferentially binds the minor groove of AT-rich DNA as an antiparallel dimer[28,29] or as a monomer.[30,31] The ability of distamycin to bind in either mode will demonstrate that HMGA1a has only a minimal effect on distamycin binding. Several groups have shown that distamycin and related polyamides are capable of regulating gene expression *in vitro* and *in vivo* by hindering the binding of transcription factors and related proteins.[32−37] For example, Grant et al. showed that the polyamide netropsin effectively displaces a polypeptide that corresponds to the second and third AT hook motifs of HMGA1 [HMGA1(2/3)] from the *NOS2* promoter DNA.[37] NMR spectroscopy showed that the addition of netropsin (at a 2:1 ratio of netropsin:protein) resulted in dissociation of HMGA(2/3) from two identical short segments of DNA, each of which had been bound by a distinct AT hook.[37]

Distamycin generally binds well to any AT-rich sequence, and a variety of methods including gel mobility shift assays,[27,33,38,39] *in vivo* studies,[33] Northern Blotting,[33,38] and footprinting[39] have shown that distamycin inhibits binding of HMGA proteins to DNA. A dynamic understanding that includes structural analysis of AT hook displacement and kinetic analysis of distamycin dissociation is the focus of our studies. Examination of the competition between distamycin and the AT hook motif by ^{1}H chemical shift and NOESY experiments has allowed for a subnucleotide, structure-based mechanism to be characterized. In the presence of distamycin,

Received: May 27, 2011
Revised: August 18, 2011
Published: August 19, 2011

the AT hook exhibits no contacts with the nitrogenous bases in either the minor or major grooves, thus showing that the AT hook is not bound within the DNA. Furthermore, by homonuclear NOESY and ^{31}P experiments, the displaced AT hook was shown to electrostatically associate with the DNA backbone, which indicates that the displaced protein is nonspecifically bound to the DNA. At high concentrations of displaced AT hook, the peptide does appear to weakly associate with nucleotides that flank the distamycin binding site. Additionally, dissociation of the first molecule of distamycin was actually slowed in the presence of excess AT hook, and the rate of dimer dissociation was not altered by the presence of the AT hook. This analysis of the fine structure and kinetics of the dynamic competition led naturally to the study of a biologically relevant full-length protein. The change in the hydrodynamic profile of a short DNA was monitored by fluorescence anisotropy to better understand binding dynamics of the displacement of HMGA1a by distamycin. Saturation of both AT hook DNA binding sites with distamycin dimers is required to drive the equilibrium completely to the dissociation of all HMGA1a:DNA complexes in the solution. It is important, due to the cooperative nature of HMGA binding, to investigate low ratios of the minor groove binder to DNA, to see whether HMGA cooperativity plays a role in its own displacement. These studies show that 1 equiv of distamycin to DNA is capable of displacing the entire protein, thus raising the possibility that targeting a single AT hook binding site (rather than the two or three that are bound by a single protein) would be sufficient to regulate HMGA1 binding and function.

MATERIALS AND METHODS

Materials and Sample Preparation. 5′-CGAAATTTCG was synthesized and desalted by Operon or Integrated DNA Technologies. This symmetrical DNA decreases the number of proton resonances by half (Figure 1A), allowing for simpler NMR spectra than with nonsymmetric DNA. A segment of DNA that corresponds to the distal negative regulatory element (DNRE) of the human interferon-A gene[40] was chosen for the studies conducted with the full-length protein. This DNA and was synthesized with a 5′-6-carboxyfluorescein tag and HPLC purified by Eurofins MWG Operon (Figure 1B). *N*-TPKRPRGRPKK (AT hook; Figure 1C) is identical to the second AT hook in HMGA1a, except for the addition of a second C-terminal lysine. The peptide was synthesized and reverse phase-HPLC purified by the W.M. Keck Facility at Yale or Biosynthesis Inc. HMGA1a protein was purchased from Abnova. Distamycin A (Figure 1D) was purchased from 3B Scientific or Sigma-Aldrich. DNA and distamycin concentrations were determined using UV−vis spectroscopy (Shimadzu Biospec-mini: dsDNA mode and ε_{304} = 36 000 M^{-1} cm^{-1}). Herein, solution mixtures will be described as ratios of distamycin:AT hook or HMGA1a:DNA (Dst:P:D).

Peptide Quantification. Peptide concentration was determined using the ATTO-TAG CBQCA kit (Invitrogen Molecular Probes).[41] A tryptophan-labeled AT hook peptide (*N*-TPKRPRGRPKK**W**) was used as the standard (ε_{280} = 5600 M^{-1} cm^{-1}). ATTO-tagged peptides were deposited on Whatman nitrocellulose membranes by filtration (dot blot; Whatman) and the fluorescence emission quantified (GE Typhoon Trio; ex 488 nm, em 555 nm). A standard curve generated with tryptophan-labeled AT hook was used to quantify the unlabeled peptide concentration.

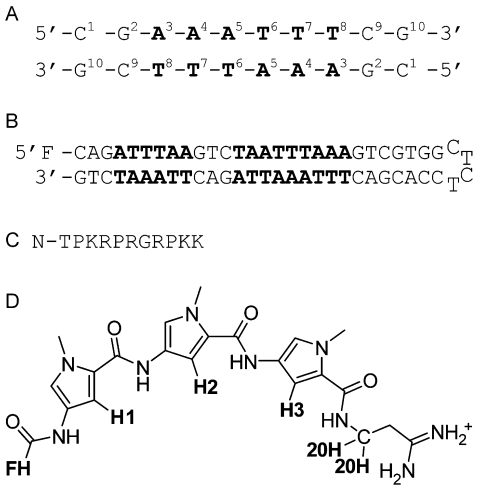

Figure 1. (A) Palindromic DNA used in NMR studies. Nucleotides are numbered relative to their 5′ location. Strands are symmetric such that, for example, protons of both G^{10} are equivalent. Cognate AT hook and distamycin binding sites are bolded. (B) 5′-carboxyfluorescein (F) tagged, hairpin DNA corresponding to the DNRE of the interferon-A gene.[40] Cognate AT hook and distamycin binding sites are boldface. (C) Peptide corresponding to the AT hook. (D) Chemical structure of distamycin A. For simplicity, "pyrrole" protons will refer to H1, H2, and H3 and not to other ring protons, which face away from the minor groove when distamycin is bound to DNA. Key protons are bolded (e.g., FH is the formyl proton).

NMR Sample Preparation. Samples were prepared in 10 mM phosphate buffer [10 mM phosphate, 100 mM Na^+ (from NaH_2PO_4, NaOH, and NaCl), 1 mM EDTA, pH 6.7], according to the molar ratios indicated in the Results section (relative to constant 200 nmol of DNA). The conditions of all NMR experiments prevented variations in pH, temperature, and buffer and salt concentrations, so that changes in chemical shifts are attributable to ligand binding events. Each sample was prepared in buffered water, lyophilized to dryness, and resuspended in either 0.5 mL of 99.9% D_2O or 0.5 mL of 9:1 H_2O:D_2O. Because of the amount of time necessary to prepare and perform individual NMR experiments (typically on the time frame of hours), each spectrum reflects a solution at equilibrium, independent of the order in which the biomolecules were added.

NMR Measurements. NMR measurements were taken at 500 MHz (Varian Inova 500) or 400 MHz (Varian MR-400) at 25 °C. 1D proton spectra (minimum 512 transients) in D_2O were collected on the MR-400 with sweep widths of 4006.4 Hz and 8207 complex points or on the Inova 500 with sweep widths of 4998.1 Hz and 10239 complex points. Proton decoupled scans (minimum 1024 transients) were collected for ^{31}P (MR-400), with a sweep width of 2431.9 Hz and 3891 complex points. Exchangeable proton measurements (MR-400) had sweep widths of 6009.6 Hz with 13 112 complex points.

The equilibrium constants for the AT hook were determined by titrating 8.45 mM peptide (10 mM phosphate buffer/D_2O) in increments of 0.1:1.0 peptide to DNA (2.77 μL/titration). Minimal broadening of resonances was observed (SI Table 2), and the K_d values were calculated from the frequency changes as a function of peptide concentration.[42]

2D NOESY in D_2O were collected on the Inova 500 (phase-sensitive States-TPPI quadrature detection; 4998.1 Hz per dimension sweep width). 128 scans were taken for each of the

256 increments in t_1 with 1024 complex points in t_2. A recycle delay of at least 1 s was used with a steady-state pulse prior to subsequent scans. 2D NOESY in 9:1 H_2O:D_2O were collected on the MR-400 (phase sensitive States-TPPI quadrature detection; 6009.6 Hz sweep width). Gradient suppression of water resonance was applied. NOESY mixing times were 150, 400, or 700 ms (only 150 ms data shown herein). 2D spectra were analyzed using SPARKY.[43]

Assignments for DNA and AT hook:DNA proton resonances (SI Table 1) were based on sequential connectivities observed in the NOESY spectra. Assignments for distamycin complexes (SI Table 1) were similarly determined and facilitated by comparison with reported assignments for distamycin complexed with a comparable DNA sequence.[29] Rates of dissociation of 1:1 distamycin:DNA (using the exchange of 5AC2 between free and bound) and dissociation of the 2:1 to the 1:1 complex (using the exchange of the pyrrole protons) were determined using equations in ref 44.

Referencing. Proton chemical shifts were referenced to trimethylsilyl propionate (TSP) or to a contaminant peak (7.99 ppm from TSP, integration is one-half of one DNA proton). The contaminant peak does not shift upon addition of AT hook or distamycin. Phosphorus chemical shifts are referenced to triphenylphosphine in $CDCl_3$ (−6.0 ppm) resuspended in a sealed tube within the experimental NMR sample.

Fluorescence Anisotropy. Titrations were conducted at 25 °C in the 10 mM phosphate buffer described above, using a Horiba Jovin Yvon FloroMax-3. All components were resuspended in the same phosphate buffer, such that buffer conditions remained constant throughout the course of each experiment. It is important to note that addition of the peptide to a fluorescently labeled hairpin DNA analogue of the DNA in Figure 1A exhibited no change in anisotropy, most likely because the change in size and shape was not sufficient to alter the anisotropy signal (data not shown). Each solution underwent 15 scans initiated 3 min after titration and concluded within 7 min after addition of titrant. Each experiment contained 22.5 pmol of DNRE in 2.00 mL (11.25 nM). For HMGA1a association experiments, 2.38 pmol of protein was added per titration (0.5 μL per titration). For distamycin association experiments, 5.41, 21.63, or 43.26 pmol of distamycin was titrated (4, 1, and 2 μL, respectively) to either free DNA or solution containing DNA and 35.7 pmol of HMGA1a. Six sets of titrations were conducted (some sets included more titration points), and data were averaged. Experimental errors were less than 4.0, 2.2, and 3.0 millianisotropy units for HMGA1a association, distamycin association, and HMGA1a dissociation, respectively.

RESULTS

Structural Analysis and Binding Affinity of AT Hook for AT-Rich DNA. Association of the AT hook peptide, *N*-TPKRPRGRPKK (Figure 1C), to the AT-rich DNA (Figure 1A) was characterized by homonuclear NOESY. Similar complexes have been structurally characterized by NMR;[45,46] however, it was important to repeat these studies for direct comparison with the competition experiments in the aforementioned solution conditions. Strong couplings were observed between the protons on the C2 of adenine (AC2) of nucleotides 4 and 5 with the β, γ, and δ protons (along with α for 5 AC2) of both core arginine residues (SI Figure 1). Therefore, the peptide is bound to the minor groove of the DNA. A single resonance is observed for each of the 3, 4, and 5 AC2 protons (7.27, 7.12, and 7.62 ppm, respectively), indicating that the Arg-Gly-Arg core of the peptide binds pseudosymmetrically to the DNA, as anticipated.[46]

Chemical shift perturbations of the nitrogenous base protons were monitored by 1D NMR upon increasing concentrations of AT hook and establish the formation and stability of the resulting complex (Figure 2A). The peptide undergoes fast exchange onto the DNA, which allows nucleotide-specific quantification of equilibrium dissociation constants by mon-

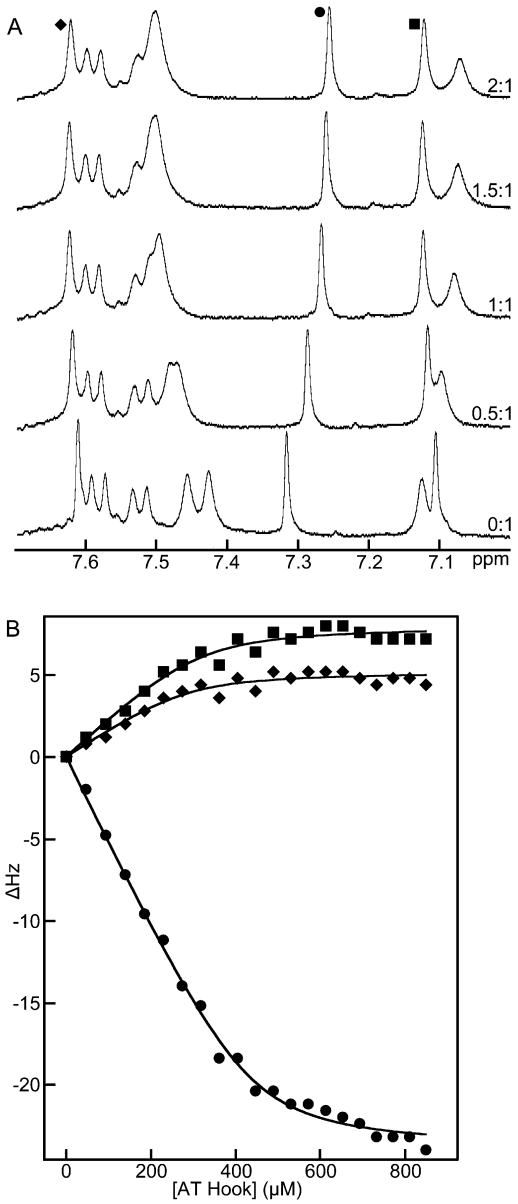

Figure 2. AC2 protons shift upon addition of AT hook. (A) 1D expansion of AC2 protons. Sample spectra are shown and the molar ratios correspond to AT hook:DNA. 3, 4, and 5 AC2 protons are denoted by circles, squares, and diamonds, respectively. (B) Changes in AC2 proton frequency as a function of AT hook concentration. Negative values correspond to upfield shifts and positive values to downfield shifts. Data were fit: $\Delta_{obs} = \Delta_{max}\{(K_d + [P]_0 + [D]_0) - ((K_d + [P]_0 + [D]_0)^2 - (4K_d[P]_0))^{1/2}\}/2[P]_0$, where $[P]_0$ and $[D]_0$ are the total concentrations of peptide and DNA at each titration point. Δ_{obs} and Δ_{max} are the changes in chemical shift in Hz for each titration point and at saturation, respectively.[42]

dx.doi.org/10.1021/bi200822c | *Biochemistry* 2011, 50, 8107–8116

itoring changes in the frequency of specific DNA protons as a function of peptide concentration. Of significant interest are AC2 protons (symbols in Figure 2A), which lie in the DNA minor groove and make direct contact with the peptide. The AC2 protons of nucleotides 4 and 5 shift downfield by 7.99 and 5.19 Hz, respectively, while 3 AC2 shifts upfield by 23.96 Hz. The large frequency change of 3 AC2 is due to the proximity of the positively charged Arg residues bound within the DNA minor groove.[46] Titration data were fit with a one to one binding isotherm, and the resultant K_d values were 17.7 ± 2.5, 25.0 ± 7.1, and 24.8 ± 9.7 μM for the 3, 4, and 5 AC2 protons, respectively (Figure 2B). K_d values determined from each nitrogenous base proton shift are mostly between 4.8 and 25.0 μM, a slightly broader range than observed for the AC2 protons (SI Table 2). The only affinities that do not lie within this range are the C5 and C6 protons of 9 C, which exhibit weaker K_d values (50 and 135 μM, respectively). The major groove protons do not directly bind the AT hook[45] and are thus indirectly affected by peptide binding. Therefore, the K_d values (17−25 μM) determined from the three AC2 protons best reflect the binding affinity of the peptide for the DNA minor groove.

The dissociation constants determined by NMR are in good agreement with the previously determined K_d value for the AT hook motif (K_d = 10 μM), which was determined by dissociation of Hoechst 33258 from the 3′-UTR of the bovine interleukin-2 DNA.[23] Because of the similarity between the previously reported K_d value and those determined by NMR, the concentrations required to perform NMR experiments are in a viable realm for monitoring the competition between distamycin and AT hook for binding DNA.

Structural Analysis of Distamycin with AT-Rich DNA. The interactions between distamycin and DNA at 2:1, 1:1, and 0.5:1 Dst:D molar ratios were probed and are the same ratios of distamycin:DNA that were monitored in the presence of AT hook (discussed in following sections). Key NOE signals in the 2:1 Dst:D mixture show interactions between the pyrrole ring protons (H1, H2, and H3) and the 4/5 AC2 protons (squared regions in SI Figure 2A). NOE couplings also indicate the proximity of pyrrole ring protons to the thymidine C1′ protons and of 20H protons to the 3/4 AC2 protons. An NOE was observed between FH and 20H of distamycin, which denotes formation of the antiparallel distamycin dimer conformation.

Nitrogenous base protons in the distamycin:DNA complexes are in slow exchange on the NMR time scale, resulting in significant line broadening and lack of peak dispersion; therefore, equilibrium binding constants for distamycin were not extracted from the NMR data. The equilibrium constant for formation of the 2:1 distamycin:A_3T_3 complex has been previously reported to be 60 nM,[47] which is 2 orders of magnitude stronger than the affinity of the AT hook for the DNA.

The 1:1 mixture of Dst:D exhibits two resonances per nitrogenous base proton, one for each strand. Despite the complexity that arises from the loss of symmetry in 1:1 Dst:DNA complex, clear NOEs denote the proximity of the pyrrole protons to the 4 AC2, 5 AC2, and TC1′ protons (squared regions in SI Figure 2B). Additionally, three cross-peaks (circled region in SI Figure 2B) indicate that each pyrrole proton is in equilibrium between two different, but stable, structural states. Comparison with the NOESY of the 2:1 complex indicates that one state corresponds to the 2:1 complex. The other correlates to the 1:1 complex.[28] Thus, distamycin exchanges between the 1:1 and 2:1 binding modes during the mixing time (150 ms) of the NOESY experiment.

In the 0.5:1 Dst:D solution, NOE peaks are observed that correspond to monomeric distamycin bound to DNA (data not shown). The pyrrole protons do not exhibit exchange peaks, signifying an absence of free distamycin in the 0.5:1 ratio. However, additional cross-peaks do indicate the DNA equilibrates between the free and bound states. For example, an exchange cross-peak is observed between 7.61 and 8.14/8.23 ppm, which corresponds to the resonances of the 5AC2 proton in free DNA and in the unsymmetric, monomeric distamycin:DNA complex, respectively. This evidence suggests there is either a static 1:1 complex or fast exchange among multiple 1:1 binding sites.[29]

Distamycin Displaces AT Hook from the DNA. One-dimensional chemical shift perturbation experiments determined which species is bound to the DNA in a solution mixture of 2:1:1 Dst:P:D (distamycin:peptide:DNA). The chemical shifts of the 2:1:1 mixture are nearly indistinguishable from those of the 2:0:1 Dst:P:D solution (Figure 3 and SI Table 1),

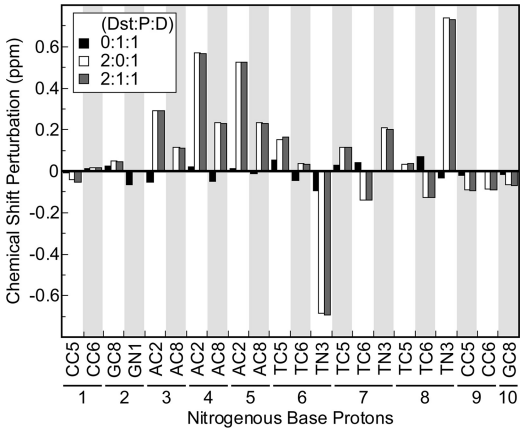

Figure 3. Chemical shift perturbations of nitrogenous base protons. All values are relative to the chemical shifts of the identical proton in the free DNA and negative values denote upfield shifts. Peak assignments are available in SI Table 1. DNA nomenclature: the number below each nucleotide position is the location of the nucleotide from the 5′-termini, the first letter is the nucleotide identity, and the second letter and number denote the atom on the nitrogenous base to which the proton is attached. 6, 7, and 8 TN3 are imino protons.

clearly showing that distamycin is bound to the DNA. For example, all three AC2 protons have equivalent resonances in the presence and absence of the AT hook.

Pyrrole ring and arginine protons exhibit distinctly different NOEs with the minor groove of DNA and are therefore good signatures for monitoring the competition between distamycin and the AT hook. The intermolecular NOEs observed in the 2:0:1 Dst:P:D complex (4/5AC2 to pyrrole, TC1′ to pyrrole, and 3AC2 to 20H) are also observed in the NOESY of the 2:1:1 Dst:P:D mixture, and Arg-DNA NOEs are not observed in this mixture (Figure 4A). In addition, the presence of the 20H-FH NOE in the 2:1:1 mixture verifies that distamycin binds as an antiparallel dimer when an equimolar concentration of AT hook (to DNA) is present. The terminal base pairs do not exhibit contacts with distamycin and are potential sites for arginine residues to associate with the DNA. However, there are no NOEs between arginine protons and any minor groove

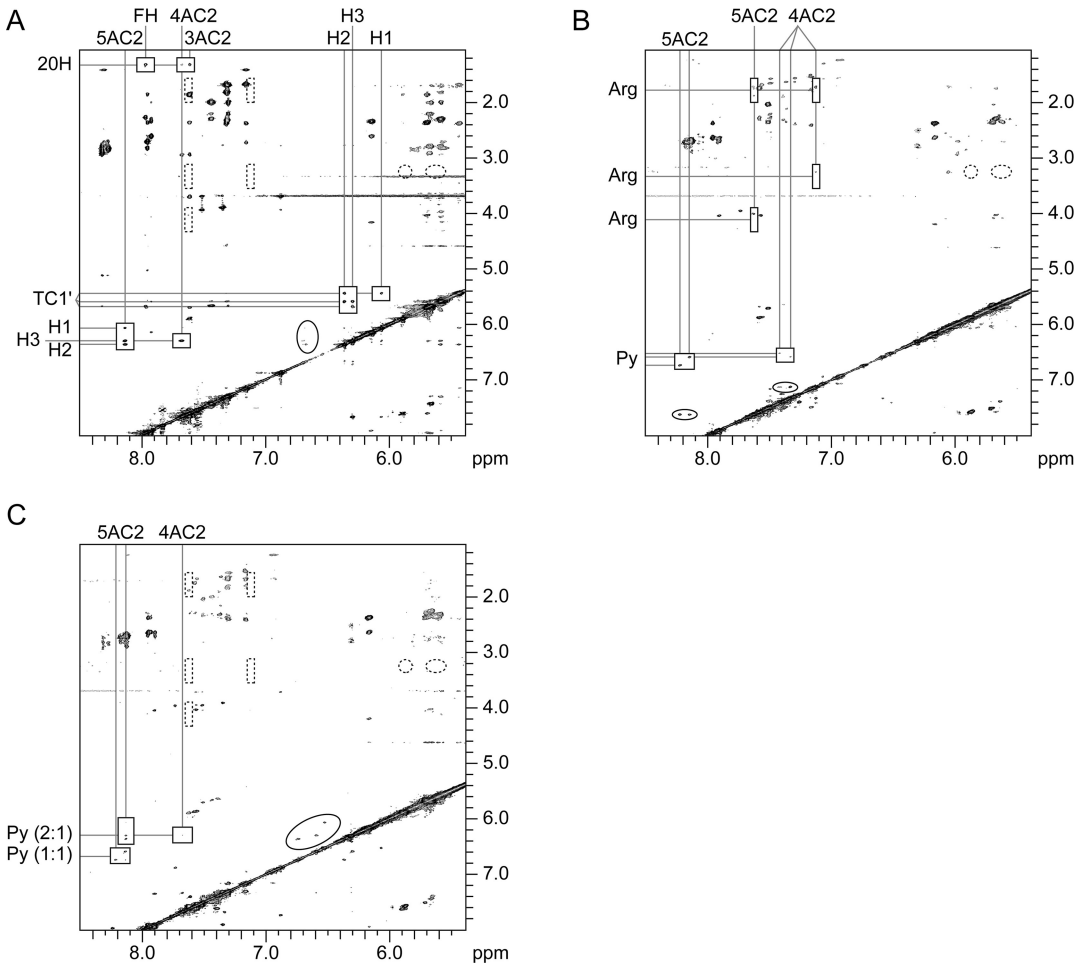

Figure 4. NOESY spectrum of Dst:P:D mixtures (150 ms mix, 25 °C). Key intermolecular NOEs are denoted with rectangles. Dashed circles correspond to regions in which new NOEs were observed only in the 2:2:1 mixture (see Figure 5). (A) 2:1:1 Dst:P:D mixture. AC2-Arg NOEs are not present (dashed rectangles), although these regions do overlap distamycin:DNA NOEs (1.6 and 1.9 ppm; SI Figure 2A). Pyrrole protons exhibit weak cross-peaks, indicating exchange between free and 2:1 distamycin:DNA states (circled region). (B) 0.5:2:1 Dst:P:D. The 4 and 5 AC2 protons exchange between the distamycin and AT hook bound forms (solid circles). While the 4/5 AC2 resonances are very similar for the free (7.10/7.61 ppm) and peptide bound (7.12/7.62 ppm) states, the exchange peaks map to the peptide bound resonances and not to the free DNA resonances. (C) 1:2:1 Dst:P:D. The Arg-AC2 NOEs are absent (dashed boxes). The pyrrole protons exchange between 1:1 and 2:1 states (solid circle).

protons in the 2:1:1 mixture. Therefore, the AT hook does not occupy the minor groove in the 2:1:1 mixture.

Small deviations (≤0.012 ppm) were observed between the 1D spectra of the 2:1:1 and the 2:0:1 mixtures (Figure 3 and SI Table 1), and the larger of these shifts were for 1 CC5 (−0.012 ppm), 6 TC5 (−0.009 ppm), and the imino protons of each T (−0.010 ppm). Perturbations of the imino protons indicate that the groove width for the distamycin bound state has been altered by the presence of the AT hook. No significant changes were observed for any other major groove proton (9CC5, 7/8 TC5, and each AC8, GC8, TC6). The unaffected major groove protons are distributed along the length of the DNA, and the other major groove protons undergo relatively small shifts in the presence of AT hook; therefore, it is very unlikely that the peptide was displaced to the major groove.

Monomeric and Dimeric Distamycin Binding in the Presence of Displaced AT Hook. NOESY was used to monitor the formation of Dst:D complexes at low ratios of distamycin in the presence of excess AT hook. In a 0.5:2:1 Dst:P:D mixture, NOEs are observed for the 4/5 AC2-arginine and the 4/5 AC2-pyrrole interactions (rectangles in Figure 4B). Additional cross-peaks (solid circles in Figure 4B) indicate exchange of the 4/5 AC2 DNA protons between protein-bound and distamycin-bound states. Therefore, the distamycin:DNA and peptide:DNA complexes are in equilibrium with each other. Pyrrole proton resonances indicate the presence of the 1:1 distamycin:DNA complex, and they do not exhibit exchange peaks with the 2:1 state, indicating that all bound distamycin is monomeric. The rate of dissociation of the 1:1 distamycin:DNA complex in the 0.5:2:1 mixture is 0.5 Hz. In the absence and presence of 1 equiv of AT hook (to DNA) the rates of 1:1 distamycin:DNA complex formation are 0.7 and 0.8 Hz, respectively. In the absence of the AT hook, the k_{off} value is in good agreement with that previously determined by stopped-flow kinetics.[48] Therefore, the dissociation of the first molecule of distamycin is only slightly slower when AT hook is in excess but is unaltered by the presence of equimolar AT hook.

In the 0.5:2:1 mixture, the AC2 protons do not exchange with free DNA resonances, indicating that there is no measurable free DNA in the sample. Together with the observation that distamycin complexes with DNA only as the monomer, these data indicate that half of the DNA molecules are bound to distamycin and the remainder are bound to the peptide in the 0.5:2:1 mixture. Therefore, monomeric

dx.doi.org/10.1021/bi200822c | *Biochemistry* 2011, 50, 8107–8116

distamycin effectively inhibits the AT hook from binding the DNA. Additionally, the DNA minor groove does not need to be widened by the addition of the second distamycin molecule to dissociate the AT hook.

Increasing the ratio of distamycin (1:2:1 Dst:P:D) results in loss of detectable NOEs between Arg and AC2 protons (dashed rectangles, Figure 4C). Additional NOEs to Arg are not observed for any DNA proton. Therefore, the AT hook is not bound to the minor or major groove of DNA. NOEs are observed for the adenine−pyrrole interactions, indicating formation of distamycin:DNA complexes (rectangles in Figure 4C). Exchange peaks are observed for the pyrrole protons (circled region Figure 4C), indicating distamycin is free to exchange between the 1:1 and 2:1 forms at the 1:2:1 ratio as it does in the 1:0:1 mixture. In the presence of 0, 1, and 2 equiv of AT hook (to DNA), the rates of dissociation from the 2:1 to the 1:1 distamycin:DNA complexes were 0.1, 0.1, and 0.2 Hz, respectively. The rate of dissociation, in the absence of AT hook, is in good agreement with the previously determined off rate for the 2:1 complex.[48] Therefore, dimer dissociation is essentially unaffected by the presence of the AT hook.

In the 1:2:1 Dst:P:D mixture, the pyrrole protons exhibit exchange between the 2:1 and 1:1 structures and do not exhibit NOE or exchangeable binding with the AT hook peptide. Additionally, the 1:2:1 and 1:0:1 Dst:P:D spectra (Figure 4C and SI Figure 2B) are similar to each other, indicating that the AT hook does not significantly alter binding of the distamycin monomer to the DNA (smaller perturbations to distamycin binding will be discussed below). Therefore, distamycin does not appear to inhibit the AT hook by directly binding and sequestering the AT hook.

AT Hook Electrostatically Shields the DNA Backbone. 1D phosphorus scans were used to probe DNA backbone interactions (SI Figure 3). The phosphorus resonances of the 2:0:1 and 0:2:1 Dst:P:D complexes have distinctly different patterns, which is not surprising due to the high density of positive charge in the peptide. The chemical shifts of the distamycin:DNA complex are more dispersed than those observed for the AT hook:DNA complex, which can be attributed to minor groove widening and untwisting of the DNA helix due to dimeric distamycin binding.[49] The 2:2:1 mixture shows a nearly identical footprint to the 2:0:1 Dst:P:D; however, resonances in the 2:2:1 mixture are shifted upfield (shifts ranged from −0.055 to −0.084 ppm). The 2:1:1 mixture exhibits smaller shifts, ranging from −0.022 to −0.037 ppm (data not shown). The relatively uniform upfield shifting of each phosphorus signal by the displaced peptide indicates that the positively charged AT hook electrostatically shields the entire phosphate backbone in a peptide concentration dependent manner. These data indicate that the displaced peptide, while not specifically bound in either the minor or major groove, does exhibit nonspecific association with the DNA backbone. Although unlikely, this nonspecific binding may allow HMGA proteins to retain function within the cell due to the conformational flexibility of the protein.

Excess AT Hook Alters the Structure of the Distamycin:DNA Complex. Increases in the AT hook concentration shift the intramolecular ^{1}H NOEs for 1C, 2G, 9C, and 10G upfield (squared regions in Figure 5). For example, 1 CC5 and 10 GC8, protons shift upfield 0.04 and 0.02 ppm, respectively, as the concentration of AT hook increased from 0 to 2 mol equiv relative to the DNA. The accompanying 1 CC2′ and 10 GC1′ protons also shift upfield

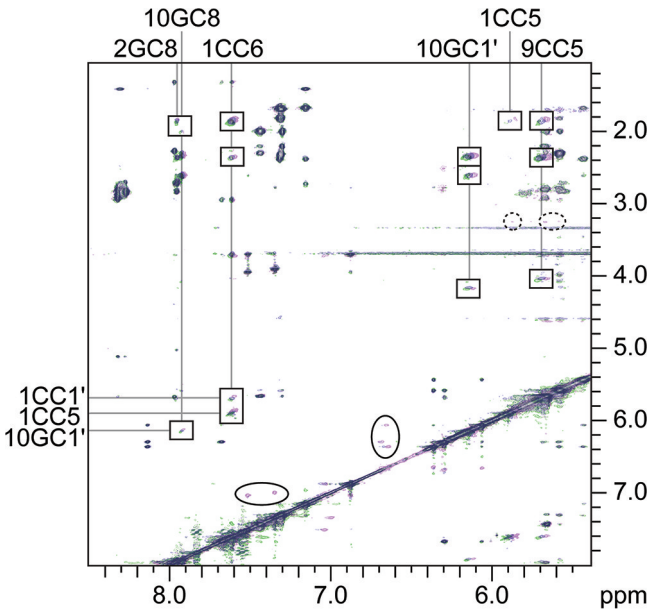

Figure 5. 2:*x*:1 Dst:P:D NOESY (150 ms mix, 25 °C). 2:0:1 (green), 2:1:1 (blue), and 2:2:1 (purple) mixtures of Dst:DNA complex. Intramolecular NOEs that shift with increasing AT hook concentrations are boxed, most of which NOE to ribose protons (1.8−4.2 ppm). The weak NOEs, which are only observed in the 2:2:1 mixture, are denoted (dashed circles). At the 2:2:1 ratio, pyrrole protons exchange between the free and bound states (solid circles). The leftmost solid circle corresponds to the *N*-methyl protons of distamycin. Cross-peaks at 6.4 and 2.5/2.8 ppm are anomalies that are visible in many of the spectra, regardless of the biomolecular solute. The pyrrole protons do not shift upon addition of the AT hook, indicating that distamycin binding is static regardless of the peptide concentration.

(0.03−0.04 ppm). The small upfield shift of the 9C NOE is presumably due to proximity of this nucleotide to the positively charged amidino tail of distamycin. The minor groove of the AT-rich region is bound by distamycin, but the altered NOEs of the terminal nucleotide protons indicate that the ends of the DNA are affected by the AT hook. In the presence of excess AT hook (2:2:1 mixture), very weak NOEs are observed for 1CC5, 9CC5, and 1CC1′ with a single proton resonance, which could be an arginine (3.3 ppm; dashed circles in Figure 5). No other nitrogenous base protons exhibit unaccounted for NOEs in excess AT hook. These new NOEs were not observed in spectra of Dst:P:D mixtures of solutions containing lower concentrations of the peptide or distamycin. Thus, in addition to shielding the entire phosphate backbone, excess amounts of the peptide may associate weakly with major (CC5) of 1C and 9C and minor (C1′) groove protons of 1C in the 2:2:1 Dst:P:D mixture. This weak association may also be the result of accessible DNA termini, allowing the peptide to wrap around the ends of the short DNA.

In the 2:2:1 mixture, there is no evidence for the binding of the AT hook to the AT-rich region of the DNA; however, cross-peaks indicate that distamycin does equilibrate between the free and bound states (circled in Figure 5). Additionally, the NOESY spectra of the 1:2:1 (Figure 4C) is similar but not identical to the 1:0:1 mixture (SI Figure 2B) as illustrated by the absence of NOEs between TC1′ and the pyrrole rings in the 1:2:1 mixture. These observations, in conjunction with the slight changes in the presence of AT hook observed by 1D (Figure 3) and NOESY (Figure 5), indicate that the displaced

dx.doi.org/10.1021/bi200822c | *Biochemistry* 2011, 50, 8107−8116

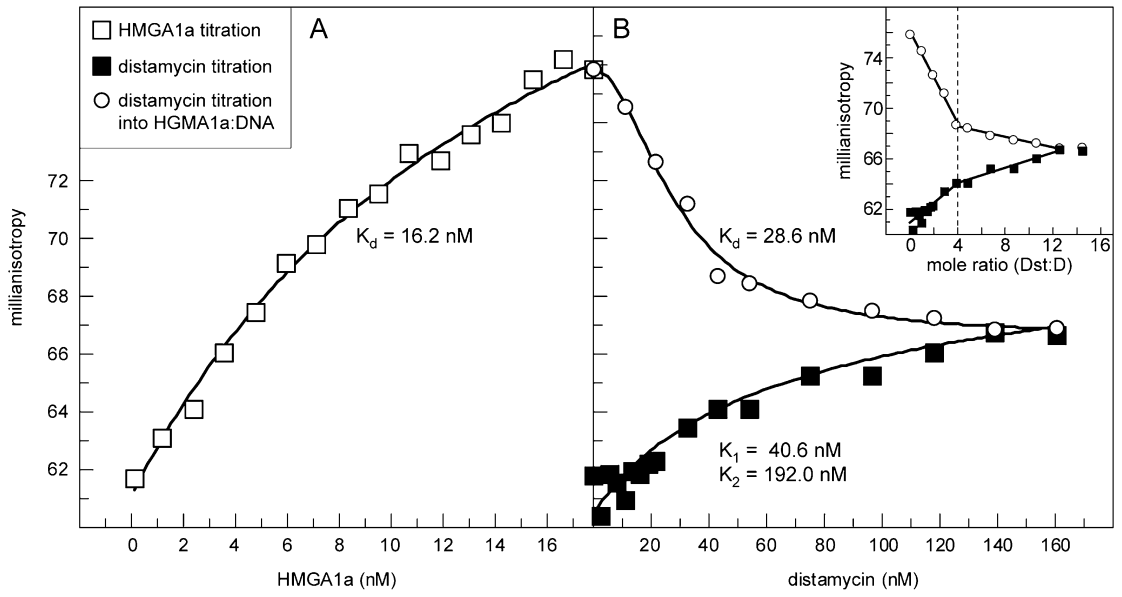

Figure 6. Fluorescence anisotropy of HMGA1a and distamycin titrated into DNRE DNA. (A) HMGA1a association data are fit with $A_0 + (A(x/(x + K_d)))$, where A_0 and A are the initial level and the total change in anisotropy levels and x is the concentration of HMGA1a. Correlation (R) for the fit is 0.9964. (B) Distamycin association (squares) and HMGA1a dissociation by distamycin (circles). Distamycin association data are fit by $A_0 + A((x/(x + K_1)) + (x/(x + K_2)))$, and HMGA1a dissociation date are fit by $A_0 - (A(x^2/(x^2 + K_d^2)))$. R values are 0.9662 and 0.9953, respectively. Inset: distamycin titrations are shown with linear fits. Both sets of data exhibit a change in slope at 4:1 (dashed line).

AT hook weakens and slightly perturbs the structure of the distamycin:DNA complex.

These NMR data identify key steps in the dissociation of the AT hook motif by distamycin. Thus, we aim to place our new structural understanding of AT hook displacement into a larger framework by studying the full-length HMGA1a protein. Interestingly, binding of the full-length HMGA1a is highly cooperative, and affinity increases by 3−4 orders of magnitude when at least two AT hook motifs exist within a single protein.[23] Fluorescence anisotropy was used to investigate the global changes in size and shape during the competition with full-length protein. The stoichiometric dependence of the change in anisotropy provides important structural insight into how distamycin perturbs the protein−DNA complex.

Dissociation of Full Length HMGA1a by Distamycin. Addition of the full-length protein to fluorescently labeled DNA results in increased anisotropy, reflecting a decrease in rotation of the fluorophore in solution. This loss of rotational freedom is due to an increase in the hydrodynamic radius of the DNA, which is coupled to HMGA1a association (Figure 6A). The data were best fit by a 1:1 binding isotherm with a K_d = 16.2 nM. This value is in agreement with previously reported K_d values of 1 and 7 nM for HMGA1a, as determined by Hoechst displacement and gel mobility shift assays, respectively.[23,27]

Titration of distamycin resulted in a smaller positive change in anisotropy (closed squares in Figure 6B). A sharp increase in anisotropy was observed up to the ratio of 4:1 Dst:DNA, which represents saturation of each of the two AT hook sites by distamycin dimers. The gradual increase in anisotropy above the 4:1 ratio indicates nonselective saturation of the entire DNA minor groove by distamycin. The data were best fit by a 2:1 binding isotherm (rather than 1:1 or 4:1), with corresponding K_{obs} values of 40.6 and 192.0 nM. The minor groove binder Hoechst 33258 exhibits cooperative binding at two adjacent locations that is minimized by the presence of a hairpin loop, which stabilizes the free DNA in the duplex form.[50] The DNA used in the anisotropy experiments herein also contains a hairpin loop; this suggests that the binding affinity of distamycin monomers to two adjacent sites can be described by a single K_{obs} and formation of both dimers by the second K_{obs}. The negative cooperativity of distamycin dimer formation[47,51] indicates that binding of the first two molecules of distamycin, each to adjacent sites, should correspond to the stronger K_{obs} (40.6 nM). Therefore, binding of the first distamycin is slightly weaker than binding of HMGA1a (16.2 nM) to the same DNA.

Distamycin was titrated into the solution of 1.6:1 HMGA1a:DNA (17.8 nM HMGA1a), which is anticipated to contain a mixture of 1:1 HMGA1a:DNA complexes and free HMGA1a (Figure 6A). Anisotropy decreased with increasing concentrations of distamycin, indicating dissociation of HMGA1a from the DNA (open circles in Figure 6B). The distamycin titration data (±HMGA1a) converge by 12:1 distamycin:DNA. Therefore, in the presence of excess protein, distamycin is bound to the DNA, and the protein is bound neither specifically nor nonspecifically to the DNA at high concentrations of distamycin. Previous studies have shown that shorter peptides corresponding to a single AT hook can result in ordered aggregation of the peptide:DNA complexes.[24] Thus, the nonspecific, electrostatic binding observed by NMR occurs only for the peptide and not the full-length protein.

Formation of Distamycin:Protein:DNA Complexes Are Not Observed. The titration of distamycin into HMGA1a:DNA likely results in an ensemble of different complexes, the ratio of which would change over the course of the titration. The 0.5:2:1 Dst:P:D mixture analyzed by NOESY NMR suggests that distamycin and the AT hook cannot bind the same region of DNA simultaneously, so it is unlikely that distamycin and the AT hooks of HMGA1a bind to the same region of the DNA. On the basis of the independent titrations of HMGA1a and distamycin (Figure 6, open and closed

dx.doi.org/10.1021/bi200822c | Biochemistry 2011, 50, 8107−8116

squares, respectively), it is likely that formation of stable ternary complexes (≥1 distamycin:1 HMGA1a:1 DNA) would result in at minimum no change and probably an increase in anisotropy, regardless of the potential ternary structures. However, at no point in the titration does the anisotropy increase (circles, Figure 6B), indicating that it is very unlikely that a significant percentage of DNA molecules stably bind both the protein and distamycin. It is possible that transient ternary complexes are formed. Ultimately, the gradual decrease reflects an ensemble of distinct distamycin:DNA and HMGA1a:DNA complexes.

Full-Length HMGA1a Alters Negative Cooperativity of Distamycin Dimerization. Distamycin dimerization exhibits negatively cooperative binding to the DNA sequences used in both the NMR and anisotropy experiments described herein. Additionally, in the presence of the AT hook (as shown by NMR in Figure 4B) the monomeric distamycin complex will predominate over the dimeric complex at low distamycin concentrations. However, distamycin binding to DNA in the presence of HMGA1a is best described by 2x distamycin + DNA ↔ distamycin$_2$·DNA, with a single K_d value (28.6 nM, Figure 6B), and the data are not well fit by an equation analogous to that used for distamycin association in the absence of HMGA1a (fit not shown). Therefore, unlike the NMR studies, where the AT hook has little effect on distamycin cooperativity, the full-length protein does diminish the cooperative binding of distamycin.

One Equivalent of Distamycin Displaces HMGA1a. In the presence of HMGA1a, distamycin binding is not cooperative; therefore, the addition of 1 equiv of distamycin to DNA (11.21 nM) is sufficiently below the K_d (28.6 nM) that the majority of the distamycin:DNA complexes that are formed will be 1:1. Remarkably, 1 equiv of distamycin results in a decrease in anisotropy from 76.0 to 74.6 millianisotropy units (16% decrease in signal). Taking into account the decrease in anisotropy due to displaced HMGA1a and the increase in anisotropy due to bound distamycin (and assuming that there are no stable ternary complexes), then approximately one-quarter of the previously bound HMGA1a is displaced by 1 equiv of distamycin to DNA. Because the data do not exhibit positive cooperativity with respect to distamycin binding (Figure 6B, open circles), the data indicate that formation of 1:1 distamycin:DNA complexes is sufficient to displace the entire protein (Figure 7). It is also important to consider the positive cooperativity of DNA binding by multiple AT hook motifs within a single HMGA protein.[23] In our conditions, binding of the AT hook is weak ($K_d \approx 20$ μM by NMR), whereas binding of the full protein is 3 orders of magnitude tighter (K_d = 16.2 nM) and stronger than monomeric distamycin binding (40.6 nM). Thus, it is possible that binding of one distamycin molecule to one AT hook binding site is sufficient to displace HMGA1a from the DNA.

However, anisotropy does not reach saturating levels at low concentrations of distamycin; therefore, the dissociation of all HMGA1a:DNA complexes requires higher concentrations of distamycin. Titrations of distamycin in the absence and presence of HMGA1a exhibit breaks at the 4:1 ratio (inset Figure 6), indicating that the majority of HMGA1a protein molecules are dissociated by the binding of two distamycin dimers (approximately three-quarters of the previously bound HMGA1a). Ultimately, saturation of the 28 base pair DNA (cognate and non-cognate sites) by distamycin is required to drive complete dissociation of the protein from all DNA molecules (Figure 7). These data show that as the concentration of distamycin increases, the equilibrium between HMGA1a:DNA and distamycin:DNA complexes favors formation of the latter.

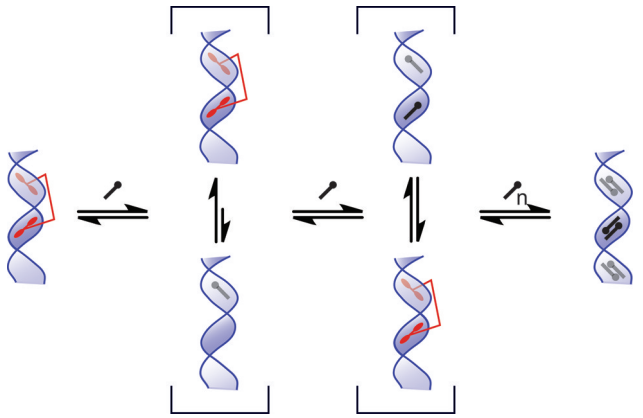

Figure 7. Possible pathway of the displacement of HMGA1a binding by distamycin. Low concentrations of distamycin (black ball and stick) can dissociate HMGA1a (binding motifs are symbolized by wings, which are connected by a line) from the DNA, but the HMGA1a:DNA complex will predominate. As the concentration of distamycin increases, the equilibrium shifts such that the HMGA1a:DNA complex is less favored. Bracketed structures are in equilibrium. Individual complexes are not meant to depict a single conformation, but an ensemble of related structures (for example, the left-most depiction of distamycin complexed with DNA is more accurately an equilibrium of different ratios of distamycin:DNA, where 1:1 predominates). *n* equals saturating amounts of distamycin.

DISCUSSION

The competition against HMGA1a and the AT hook by distamycin have been monitored using NMR and fluorescence anisotropy. These studies provide a molecular description of protein displacement by distamycin.

Formation of the distamycin:DNA complexes, first as 1:1 and then as 2:1 complexes, coincide with the displacement of AT hook and are documented by changes in NOEs between key protons of each biomolecule. The NMR data indicate that DNA preferentially binds to a single molecule of distamycin, displacing the peptide, even when the concentration of AT hook is in excess of distamycin (0.5:2:1 Dst:P:D mixture). With the exception of very weak interactions at the DNA termini when AT hook is in excess, stable ternary complexes are not formed. Therefore, the DNA equilibrates between the distamycin:DNA and the AT hook:DNA complexes, as observed in the 0.5:2:1 mixture (Figure 4B). The distamycin:DNA and HMGA1a:DNA complexes also equilibrate (as judged by anisotropy) and stable ternary complexes are also not formed. We have shown that low concentrations of distamycin are capable of promoting dissociation of the full-length protein. Therefore, it is possible that HMGA1a can be displaced by small molecules designed to selectively bind a single AT hook binding site, thereby taking advantage of the cooperative nature of HMGA1a binding.

Both the AT hook and HMGA1a alter the binding of distamycin to DNA, clearly illustrating the interplay that must exist between these two molecules that are capable of binding the same region of DNA. The 2:1 distamycin:DNA complex is weakened, and the adjacent nucleotides are structurally perturbed in the presence of the AT hook peptide (Figures 3 and 5). Interestingly, the rate of 1:1 distamycin complex

dissociation is not altered by equimolar AT hook and is actually slightly slowed by excess AT hook. The rate of forming the 1:1 from the 2:1 complex is independent of the presence of the AT hook. The AT hook does electrostatically associate with the DNA backbone, and shielding of the phosphate backbone charges may explain the altered binding by distamycin. However, this nonspecific binding was not observed with the full-length protein and has been reported to be a function of the peptide.[24] HMGA1a does, however, abolish the negatively cooperative binding that distamycin exhibits in the absence of the protein. Therefore, each molecule of distamycin binds to the DNA with equal affinity, indicating that the DNA is uniformly accessible to these molecules and that the minor groove does not need to widen for the distamycin dimers to form. These changes to distamycin binding highlight the importance of investigating the structural dynamics, in the presence of the protein, of this very well characterized small molecule.

This research has focused on the HMGA1a protein and thus provides the foundation of understanding the entire HMGA family. When attempting to target discrete sites of DNA, creation of minor groove binding molecules that inhibit a single AT hook will be paramount to creating more potent HGMA inhibitors.

■ ASSOCIATED CONTENT

Supporting Information

Supporting NOESY and ^{31}P spectra, a table of DNA and distamycin proton resonances, and a table of AT hook dissociation constants. This material is available free of charge via the Internet at http://pubs.acs.org.

■ AUTHOR INFORMATION

Corresponding Author

*Tel: (864) 294-2683. Fax: (864) 294-3559. E-mail: karen.buchmueller@furman.edu.

Funding

This work was supported by the National Science Foundation's Research Experience for Undergraduates [NSF-0648964].

■ ACKNOWLEDGMENTS

We thank Bidisha Sengupta, Natalya Degtyareva, and Jeffrey Petty for their guidance with the fluorescence anisotropy. We also thank Jeffrey Petty and Eli Hestermann for their helpful discussions.

■ ABBREVIATIONS

HMGA1, High Mobility Group A1; HMGA1a, High Mobility Group A1a; NOESY, nuclear Overhauser effect spectroscopy; AT, adenine thymine; DNRE, distal negative regulatory element; Dst:P:D, ratio of distamycin:peptide or protein:DNA; TSP, trimethylsilyl propionate; AC2, carbon 2 (C2) of adenine [same nomenclature for all DNA residues]; 3′-UTR, 3′-untranslated region; Hz, hertz; NOS2, nitric oxide synthase 2; TPPI, time proportional phase increment; FH, formyl hydrogen.

■ REFERENCES

(1) Heron, M., Hoyert, D., Murphy, S., Xu, J., Kochanek, K., and Tejada-Vera, B. (2009) *Natl. Vital Stat. Rep.*, .

(2) Pandolfi, P. P. (2001) Transcription Therapy for Cancer. *Oncogene 20*, 3116−3127.

(3) Abe, N., Watanabe, T., Izumisato, Y., Masaki, T., Mori, T., Sugiyama, M., Chiappetta, G., Fusco, A., Fujioka, Y., and Atomi, Y. (2002) Diagnostic Significance of High Mobility Group I(Y) Protein Expression in Intraductal Papillary Mucinous Tumors of the Pancreas. *Pancreas 25*, 198−204.

(4) Abe, N., Watanabe, T., Masaki, T., Mori, T., Sugiyama, M., Uchimura, H., Fujioka, Y., Chiappetta, G., Fusco, A., and Atomi, Y. (2000) Pancreatic Duct Cell Carcinomas Express High Levels of High Mobility Group I(Y) Proteins. *Cancer Res. 60*, 3117−3122.

(5) Chiappetta, G., Bandiera, A., Berlingieri, M. T., Visconti, R., Manfioletti, G., Battista, S., Martinez-Tello, F. J., Santoro, M., Giancotti, V., and Fusco, A. (1995) The Expression of the High Mobility Group HMGI (Y) Proteins Correlates with the Malignant Phenotype of Human Thyroid Neoplasias. *Oncogene 10*, 1307−1314.

(6) Flohr, A. M., Rogalla, P., Bonk, U., Puettmann, B., Buerger, H., Gohla, G., Packeisen, J., Wosniok, W., Loeschke, S., and Bullerdiek, J. (2003) High Mobility Group Protein HMGA1 Expression in Breast Cancer Reveals a Positive Correlation with Tumour Grade. *Histol. Histopathol. 18*, 999−1004.

(7) Treff, N. R., Dement, G. A., Adair, J. E., Britt, R. L., Nie, R., Shima, J. E., Taylor, W. E., and Reeves, R. (2004) Human KIT Ligand Promoter is Positively Regulated by HMGA1 in Breast and Ovarian Cancer Cells. *Oncogene 23*, 8557−8562.

(8) Treff, N. R., Pouchnik, D., Dement, G. A., Britt, R. L., and Reeves, R. (2004) High-Mobility Group A1a Protein Regulates Ras/ERK Signaling in MCF-7 Human Breast Cancer Cells. *Oncogene 23*, 777−785.

(9) Chiappetta, G., Botti, G., Monaco, M., Pasquinelli, R., Pentimalli, F., Di Bonito, M., D'Aiuto, G., Fedele, M., Iuliano, R., Palmieri, E. A., Pierantoni, G. M., Giancotti, V., and Fusco, A. (2004) HMGA1 Protein Overexpression in Human Breast Carcinomas: Correlation with ErbB2 Expression. *Clin. Cancer Res. 10*, 7637−7644.

(10) Chiappetta, G., Ottaiano, A., Vuttariello, E., Monaco, M., Galdiero, F., Gallipoli, A., Pilotti, S., Jodice, G., Siranoush, M., Colombo, M., Ripamonti, C. B., Pallante, P. L., Radice, P., and Fusco, A. (2010) HMGA1 Protein Expression in Familial Breast Carcinoma Patients. *Eur. J. Cancer 46*, 332−339.

(11) Chiappetta, G., Avantaggiato, V., Visconti, R., Fedele, M., Battista, S., Trapasso, F., Merciai, B. M., Fidanza, V., Giancotti, V., Santoro, M., Simeone, A., and Fusco, A. (1996) High Level Expression of the HMGI (Y) Gene during Embryonic Development. *Oncogene 13*, 2439−2446.

(12) Zhou, X., Benson, K. F., Ashar, H. R., and Chada, K. (1995) Mutation Responsible for the Mouse Pygmy Phenotype in the Developmentally Regulated Factor HMGI-C. *Nature 376*, 771−774.

(13) Fusco, A., and Fedele, M. (2007) Roles of HMGA Proteins in Cancer. *Nat. Rev. Cancer 7*, 899−910.

(14) Bussemakers, M. J., van de Ven, W. J., Debruyne, F. M., and Schalken, J. A. (1991) Identification of High Mobility Group Protein I(Y) as Potential Progression Marker for Prostate Cancer by Differential Hybridization Analysis. *Cancer Res. 51*, 606−611.

(15) Giancotti, V., Berlingieri, M. T., DiFiore, P. P., Fusco, A., Vecchio, G., and Crane-Robinson, C. (1985) Changes in Nuclear Proteins on Transformation of Rat Epithelial Thyroid Cells by a Murine Sarcoma Retrovirus. *Cancer Res. 45*, 6051−6057.

(16) Giancotti, V., Buratti, E., Perissin, L., Zorzet, S., Balmain, A., Portella, G., Fusco, A., and Goodwin, G. H. (1989) Analysis of the HMGI Nuclear Proteins in Mouse Neoplastic Cells Induced by Different Procedures. *Exp. Cell Res. 184*, 538−545.

(17) Reeves, R. (2001) Molecular Biology of HMGA Proteins: Hubs of Nuclear Function. *Gene 277*, 63−81.

(18) Tallini, G., and Dal Cin, P. (1999) HMGI(Y) and HMGI-C Dysregulation: A Common Occurrence in Human Tumors. *Adv. Anat. Pathol. 6*, 237−246.

(19) Yuan, S., Pan, Q., Fu, C., and Bi, Z. (2011) Silencing of HMGA1 Expression by RNA Interference Suppresses Growth of Osteogenic Sarcoma. *Mol. Cell. Biochem. 355*, 281−287.

(20) Cleynen, I., and Van de Ven, W. J. (2008) The HMGA Proteins: A Myriad of Functions (Review). *Int. J. Oncol. 32*, 289−305.

(21) Reeves, R., and Beckerbauer, L. (2001) HMGI/Y Proteins: Flexible Regulators of Transcription and Chromatin Structure. *Biochim. Biophys. Acta 1519*, 13−29.
(22) Bustin, M. (1999) Regulation of DNA-Dependent Activities by the Functional Motifs of the High-Mobility-Group Chromosomal Proteins. *Mol. Cell. Biol. 19*, 5237−5246.
(23) Reeves, R., and Nissen, M. S. (1990) The A.T-DNA-Binding Domain of Mammalian High Mobility Group I Chromosomal Proteins. A Novel Peptide Motif for Recognizing DNA Structure. *J. Biol. Chem. 265*, 8573−8582.
(24) Slama-Schwok, A., Zakrzewska, K., Leger, G., Leroux, Y., Takahashi, M., Kas, E., and Debey, P. (2000) Structural Changes Induced by Binding of the High-Mobility Group I Protein to a Mouse Satellite DNA Sequence. *Biophys. J. 78*, 2543−2559.
(25) Dervan, P. B. (1986) Design of Sequence-Specific DNA-Binding Molecules. *Science 232*, 464−471.
(26) Reeves, R., and Beckerbauer, L. M. (2003) HMGA Proteins as Therapeutic Drug Targets. *Prog. Cell Cycle Res. 5*, 279−286.
(27) Radic, M. Z., Saghbini, M., Elton, T. S., Reeves, R., and Hamkalo, B. A. (1992) Hoechst 33258, Distamycin A, and High Mobility Group Protein I (HMG-I) Compete for Binding to Mouse Satellite DNA. *Chromosoma 101*, 602−608.
(28) Pelton, J. G., and Wemmer, D. E. (1989) Structural Characterization of a 2:1 Distamycin A.d(CGCAAATTGGC) Complex by Two-Dimensional NMR. *Proc. Natl. Acad. Sci. U. S. A. 86*, 5723−5727.
(29) Pelton, J. G., and Wemmer, D. E. (1990) Binding Modes of Distamycin A with d(CGCAAATTTGCG)2 Determined by Two-Dimensional NMR. *J. Am. Chem. Soc. 112*, 1393−1399.
(30) Klevit, R.E., Wemmer, D. E., and Reid, B. R. (1986) 1H NMR Studies on the Interaction between Distamycin A and a Symmetrical DNA Dodecamer. *Biochemistry 25*, 3296−3303.
(31) Pelton, J. G., and Wemmer, D. E. (1988) Structural Modeling of the Distamycin A-d(CGCGAATTCGCG)2 Complex using 2D NMR and Molecular Mechanics. *Biochemistry 27*, 8088−8096.
(32) Nickols, N.G., and Dervan, P. B. (2007) Suppression of Androgen Receptor-Mediated Gene Expression by a Sequence-Specific DNA-Binding Polyamide. *Proc. Natl. Acad. Sci. U. S. A. 104*, 10418−10423.
(33) Baron, R. M., Carvajal, I. M., Liu, X., Okabe, R. O., Fredenburgh, L. E., Macias, A. A., Chen, Y. H., Ejima, K., Layne, M. D., and Perrella, M. A. (2004) Reduction of Nitric Oxide Synthase 2 Expression by Distamycin A Improves Survival from Endotoxemia. *J. Immunol. 173*, 4147−4153.
(34) Melander, C., Burnett, R., and Gottesfeld, J. M. (2004) Regulation of Gene Expression with Pyrrole-Imidazole Polyamides. *J. Biotechnol. 112*, 195−220.
(35) Olenyuk, B. Z., Zhang, G. J., Klco, J. M., Nickols, N. G., Kaelin, W. G. Jr, and Dervan, P. B. (2004) Inhibition of Vascular Endothelial Growth Factor with a Sequence-Specific Hypoxia Response Element Antagonist. *Proc. Natl. Acad. Sci. U. S. A. 101*, 16768−16773.
(36) Hochhauser, D., Kotecha, M., O'hare, C., Morris, P. J., Hartley, J. M., Taherbhai, Z., Harris, D., Forni, C., Mantovani, R., Lee, M., and Hartley, J. A. (2007) Modulation of Topoisomerase IIalpha Expression by a DNA Sequence-Specific Polyamide. *Mol. Cancer Ther. 6*, 346−354.
(37) Grant, M. A., Baron, R. M., Macias, A. A., Layne, M. D., Perrella, M. A., and Rigby, A. C. (2009) Netropsin Improves Survival from Endotoxaemia by Disrupting HMGA1 Binding to the NOS2 Promoter. *Biochem. J. 418*, 103−112.
(38) Baron, R. M., Lopez-Guzman, S., Riascos, D. F., Macias, A. A., Layne, M. D., Cheng, G., Harris, C., Chung, S. W., Reeves, R., von Andrian, U. H., and Perrella, M. A. (2010) Distamycin A Inhibits HMGA1-Binding to the P-Selectin Promoter and Attenuates Lung and Liver Inflammation during Murine Endotoxemia. *PLoS One 5*, e10656.
(39) Wegner, M., and Grummt, F. (1990) Netropsin, Distamycin and Berenil Interact Differentially with a High-Affinity Binding Site for the High Mobility Group Protein HMG-I. *Biochem. Biophys. Res. Commun. 166*, 1110−1117.
(40) Lopez, S., Reeves, R., Island, M. L., Bandu, M. T., Christeff, N., Doly, J., and Navarro, S. (1997) Silencer Activity in the Interferon-A Gene Promoters. *J. Biol. Chem. 272*, 22788−22799.
(41) You, W. W., Haugland, R. P., Ryan, D. K., and Haugland, R. P. (1997) 3-(4-Carboxybenzoyl)Quinoline-2-Carboxaldehyde, a Reagent with Broad Dynamic Range for the Assay of Proteins and Lipoproteins in Solution. *Anal. Biochem. 244*, 277−282.
(42) Fielding, L. (2003) NMR Methods for the Determination of Protein-Ligand Dissociation Constants. *Curr. Top. Med. Chem. 3*, 39−53.
(43) Goddard, T. D., Kneller, D. G. SPARKY 3.
(44) Bodenhausen, G. E. R. R. (1982) Direct Determination of Rate Constants of Slow Dynamic Processes by Two-Dimensional "Accordion" Spectroscopy in Nuclear Magnetic Resonance. *J. Am. Chem. Soc. 104*, 1304−1309.
(45) Huth, J. R., Bewley, C. A., Nissen, M. S., Evans, J. N., Reeves, R., Gronenborn, A. M., and Clore, G. M. (1997) The Solution Structure of an HMG-I(Y)-DNA Complex Defines a New Architectural Minor Groove Binding Motif. *Nat. Struct. Biol. 4*, 657−665.
(46) Geierstanger, B. H., Volkman, B. F., Kremer, W., and Wemmer, D. E. (1994) Short Peptide Fragments Derived from HMG-I/Y Proteins Bind Specifically to the Minor Groove of DNA. *Biochemistry 33*, 5347−5355.
(47) Lacy, E. R., Cox, K. K., Wilson, W. D., and Lee, M. (2002) Recognition of T*G Mismatched Base Pairs in DNA by Stacked Imidazole-Containing Polyamides: Surface Plasmon Resonance and Circular Dichroism Studies. *Nucleic Acids Res. 30*, 1834−1841.
(48) Baliga, R., and Crothers, D. M. (2000) On the Kinetics of Distamycin Binding to its Target Sites on Duplex DNA. *Proc. Natl. Acad. Sci. U. S. A. 97*, 7814−7818.
(49) Gorenstein, D. G. (1992) 31P NMR of DNA. *Methods Enzymol. 211*, 254−286.
(50) Rahimian, M., Miao, Y., and Wilson, W. D. (2008) Influence of DNA Structure on Adjacent Site Cooperative Binding. *J. Phys. Chem. B 112*, 8770−8778.
(51) Lacy, E. R., Le, N. M., Price, C. A., Lee, M., and Wilson, W. D. (2002) Influence of a Terminal Formamido Group on the Sequence Recognition of DNA by Polyamides. *J. Am. Chem. Soc. 124*, 2153−2163.